POTASSIUM-ARGON AGE DETERMINATION

by

Donna Davis

Accepted

R. J. Fleck

INTRODUCTION

The objective of this senior thesis was to determine the age of a rock sample from Antarctica by making a potassium - argon age determination of a biotite concentrate separated from the rock.

Location and Petrography

The sample was a granite from the Cloudmaker, a mountain on the north side of Beardmore glacier, (see Figure 1). The Cloudmaker is part of the Queen Alexandra Range of the Trans-Antarctic Mountains. The longitude of the site is 169°00'00''E and the latitude of the site is 84°15'S.

The sample is a fine- to medium-grained porphyritic quartz-monzonite. Approximately 30 percent of the rock consists of anhedral quartz grains with a distinct, undulose extinction. The size range of most quartz crystals is between 1.4 mm by 2.12 mm and 2.82 mm by 3.53 mm. Feldspar, representing approximately 55% of the total rock, is composed of 55% microcline, and 45% plagioclase. Subhedral crystals of microcline form most of the large phenocrysts. The phenocrysts, approximately 7.1 mm by 6.3 mm, have been slightly altered to sericite. The plagioclase consists of lath-shaped, subhedral crystals, with well-developed albite twinning. Most of the large phenocrysts of feldspar are zoned, but the smaller crystals are not. While the large phenocrysts are about

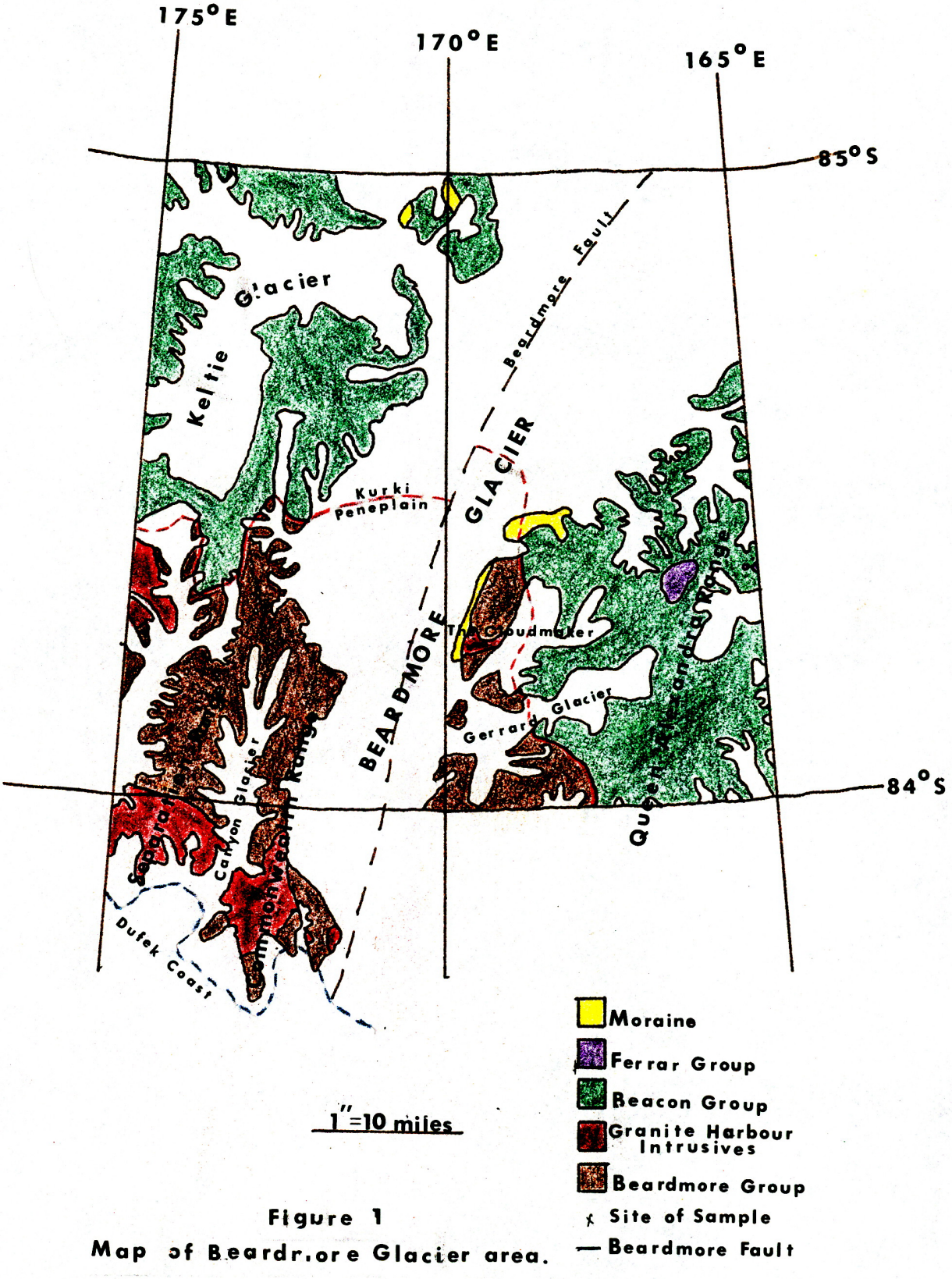

Figure 1
Map of Beardmore Glacier area.

5.65 mm by 3.18 mm, the average grain size is 3.18 mm by 1.06 mm. Some of the plagioclase has been partially altered to sericite. Between 2 and 3 percent of the feldspar has been altered to sericite. Biotite and chlorite compose 10 to 12 percent of the rock. The biotite forms subhedral to anhedral, dark brown crystals. Fully half of the biotite has been altered to chlorite. Biotite and chlorite are found together in every gradation from unaltered biotite crystals to pseudomorphs of chlorite after biotite. Most crystals are composed of slightly chloritized biotite. The chlorite is dark green on color. The size range of the biotite and chlorite crystals is 1.42 mm by 2.85 mm. Subhedral to anhedral ziron crystals 1.24 mm by .30 mm and smaller compose less than one-half percent of the total. The remaining 1.5 percent consists of magnetite, sphene, and alteration calcite.

STRATIGRAPHY

The rocks of the Queen Alexandra Range can be divided into three subdivisions. The first consists of the basement complex of Upper Precambrian and Lower Paleozoic metavolcanic, metasedimentary, and intrusive igneous rocks. The second subdivision is composed of flat-lying Upper Paleozoic and Lower Mesozoic continental sedimentary rocks, and of Jurassis intrusive dolerite sheets and co-magmatic flood basalts. The third subdivision is Pleistocene glacial deposits.

The basement complex is represented by the Goldie Formation of the Beardmore Group, and by the Hope Granite of the Granite Harbour Intrusives. The Cambrian Byrd Group,

which rests unconformably on the Beardmore Group and which is also intruded by the Hope Granite, has not been observed in the Queen Alexandra Range so far. The Goldie Formation consists of Upper Precambrian metagraywackes, argillites, phyllites, and hornfelses. The Middle Canbrian Shackelton Limestone of the Byrd Group, which overlies the Goldie Formation unconformably elsewhere, has not been observed in the Queen Alexandra Range. Shackleton Limestone has been observed in the lateral moraines in the area, however. The Hope Granite is an unfoliated, porphyritic to equigranular, microline, biotite granite of magmatic origin. With associated pegmatite and aplite dikes the granite intrudes the pre-Devonian rocks. Potassium-argon ages for the Hope Granite are mainly Ordovician (McDougall and Grindley, 1965).

The basement complex is separated from the overlying Upper Paleozoic and Lower Mesozoic rocks by the Kurki Peneplain, a nearly level erosion surface truncating the basement complex. The Upper Paleozoic and Lower Mesozoic rocks are divided into the Beacon and Ferrar Groups. The Beacon Group is composed of nearly 2,000 meters of continental sediments including tillite. The Ferrar Group consists of tholeiitic dolerites, intruding the Triassic and Permian rocks of the Beacon Groups as sills, and of co-magmatic flood basalts, totaling approximately 500 meters in thickness.

Uncompacted and only sightly weathered Pleistocene lateral and recessional moraines are common at higher altitudes in the upper reaches of Beardmore Glacier and in the deglaciated Darwin dry valleys. Striated pavements and

weathered tills found in the Miller Range, at the mouth of the Beardmore Glacier, and in the Darwin dry valleys indicate earlier deglaciation in those areas.

STRUCTURE

The rocks of the Beardmore Group are folded with subvertical to steeply eastward-dipping axial surfaces. The regional trend of the folds is north-northwest. Axial plane cleavage or schistosity is common. Most of the folding is believed to have taken place during the Ross Orogeny in Cambro-Ordovician time, prior to intrusion of post-tectonic granite during the Ordovician period. High-angle reverse faulting followed folding.

THE METHOD OF AGE DETERMINATION

The method of age determination may be divided into three steps; 1) preparation of the sample, 2) extraction and measurement of the abundance of radiogenic argon, and 3) measurement of the potassium concentration.

Biotite was the mineral selected for the age determination. The microline present in the rock was not used, since microcline does not retain argon well even at room temperature. Plagioclase contains less potassium than biotite and requires a larger sample to produce as much argon during extraction. This additional sample produces more atmospheric argon, reducing precision. Biotite is also the mineral most easily separated from a granite and preparation time is saved by its use.

Sample Preparation

First the rock was crushed by two crushers. The first, a jaw-crusher, broke the rock into small fragments, which the disc grinder broke into particles ready for sieving. The particles were sieved through Tyler mesh sizes 16, 28, 42, and 60. Size fraction 28 to 42 was used in the age determination, since it had the greatest concentration of biotite grains uncombined with grains of other minerals.

After the rock was crushed and sieved, bromoform with a specific gravity of 2.88 was used to separate the heavier biotite grains from the lighter feldspar, quartz and combined grains. The sample was poured into a bromoform-filled funnel closed at the bottom by a clamp. After the biotite

and any other heavy minerals present settled to the bottom of the funnel, the low-density fraction was removed from the surface of the bromoform, and the clamp was then opened to allow removal of the biotite. After all the sample had undergone heavy-liquid separation, the concentrated biotite was washed with acetone to remove the bromoform and then dried in the oven.

The sample was then ready for further purification by paper shaking. The purpose of the paper shaking was to separate the flatter biotite grains from the more equant impurities, such as magnetite, quartz, feldspar, hornblende, and aggregates of grains. To accomplish this, a small amount of sample is sprinkled on a stiff piece of paper, and the paper is gently shaked back and forth, while held at a low angle. The equant impurities roll off the paper, while the flatter biotite grains remain. A few thick books of biotite are also lost, but not in significant amounts.

To remove any impurities still remaining in the sample after heavy-liquid separation and paper shaking, hand-picking was necessary. A small amount of sample is sprinkled on a piece of paper divided into squares. Each of the squares is examined under a microscope and the impurities are removed with a brush. After all the sample had undergone hand-picking, the fraction left contained only pure biotite and was ready for argon and potassium analyses.

Argon Extraction and Measurement

The ^{40}Ar content of the biotite was determined to removing the argon from the biotite and mixing it with an argon spike or tracer of known isotopic composition. The relative abundance of the isotopes of argon were then measured with a mass spectrometer.

Argon Extraction

Before the biotite could be placed in the argon extraction line, several preliminary steps had to be carried out. A small clear glass bottle was weighed empty in a Mettler balance, and then reweighed containing a small amount of biotite sample. The weight of the empty glass bottle (5.00906 grams) was substracted from the weight of the bottle plus the biotite (5.08152 grams), giving the sample weight (.07246 grams). This small amount of biotite was used to avoid flooding the system with ^{40}Ar since the sample was believed to be quite old.

After weighing, the sample was placed in a molybdenum crucible, which was hung in a pyrex sample bottle. The pyrex sample bottle, the tracer (^{38}Ar), and a sample take-off tube were then attached to the argon extraction line (see Fig. 2). The tracer was prepared commercially by a manifold system, in which tracers are made in large batches. Next the argon extraction system was evacuated and baked overnight. The system was allowed to cool and was checked for leaks. The total pressure in the argon extraction line was 1.5×10^{-7} torr. The valves to the pumping system were then closed.

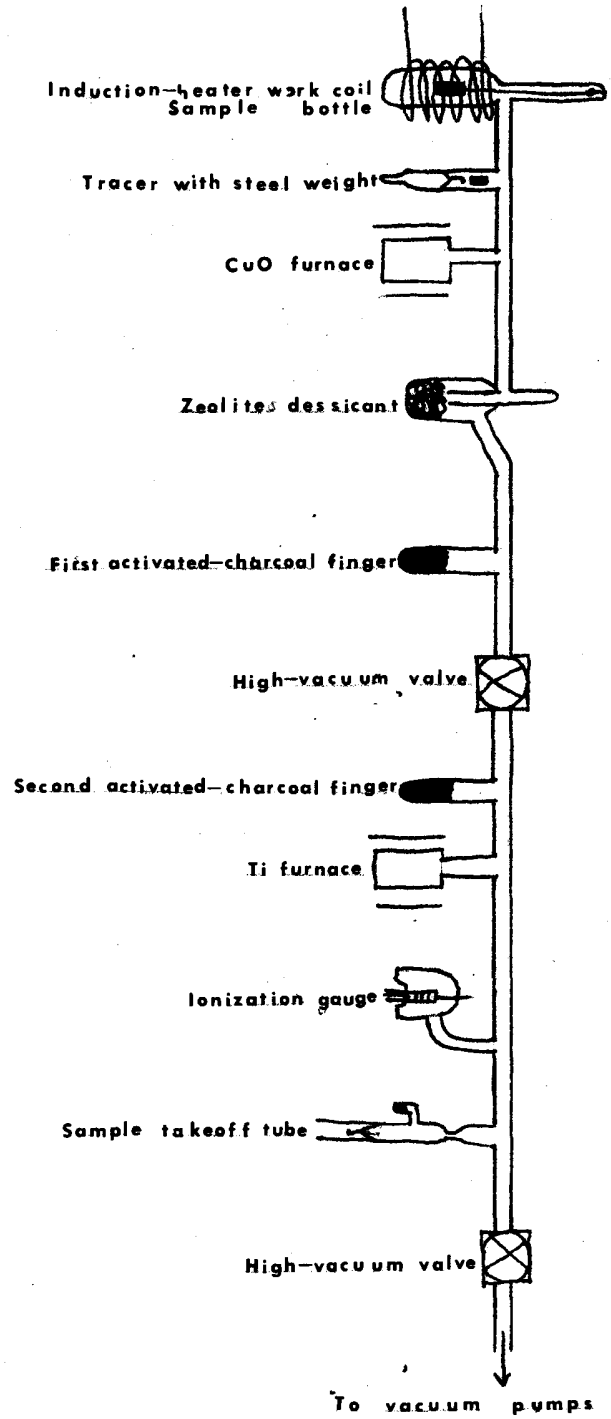

Figure 2
Schematic diagram of an argon extraction system.

Following the evacuation of the system, and the check for leaks, the extraction itself was begun. The coil of an induction heater was placed around the sample bottle, and the sample was fused. During the fusing of the sample, the outer surface of the sample bottle was cooled by a flow of forced air. When the maximum temperature (about 1500°C) was reached during the fusion process, the tracer was introduced into the system by lifting a weight with two magnets and dropping it onto the breakoff tip. While the fusion process took place, the gas was collected on the first activated charcoal finger, which was immersed in a beaker of liquid nitrogen, in order to keep the pressure in the system low. After fusion had been completed at approximately 1500°C the system was allowed to cool. The beaker of liquid nitrogen was removed and the finger of activated charcoal was allowed to warm, releasing the adsorbed gas. The released gas was exposed to copper and copper oxide at a temperature of approximately 700°C. Any hydrocarbons in the gas were ignited or oxidized and the hydrogen was oxidized to H_2O. Oxygen reacted with the copper metal, forming CuO. Water was adsorbed by a zeolite desicant.

The first high vacuum valve was opened when all the H_2, O_2, and H_2O were removed, and the gas was transferred to the second half of the extraction line. The gas was transferred by immersing the second activated charcoal finger in liquid nitrogen. The valve was then shut, and the second activated charcoal finger was allowed to warm. The gas released by the finger was exposed to hot titanium

metal, which removed all the remaining reactive gases, largely N_2. After the titanium cooled, the remaining gas, which was largely pure argon with small quantities of some of the other inert gases, was collected. The gas was collected by immersing the small activated charcoal finger on the take-off tube in liquid nitrogen for approximately 20 minutes. The sample take-off tube was then sealed and removed from the extraction line for later analysis on a mass spectrometer.

Mass Spectrometry

The sample take-off filled with the spiked argon sample was attached to the sample system of the mass spectrometer, which was then evacuated. The pressure in the mass spectrometer as measured by the ionization gauge was 10^{-9} torr. To release the gas into the mass spectrometer, the tip of the sample take-off tube was broken by lifting a weight with a magnet, and then letting it drop on the breakoff tip of the tube. The first valve was opened (see Fig.3) and the gas was allowed to equilibrate. Next the second valve was opened, introducing the gas into the ionization chamber in the source of the mass spectrometer.

In the ionization chamber electrons driven off the filament are attracted to the anode (see Fig.4). As the electrons move to the anode, they collide with the argon gas, which enters perpendicular to the anode. By colliding with the electrons, the argon gas is ionized. These positive ions are drawn out of the chamber by the weak field between

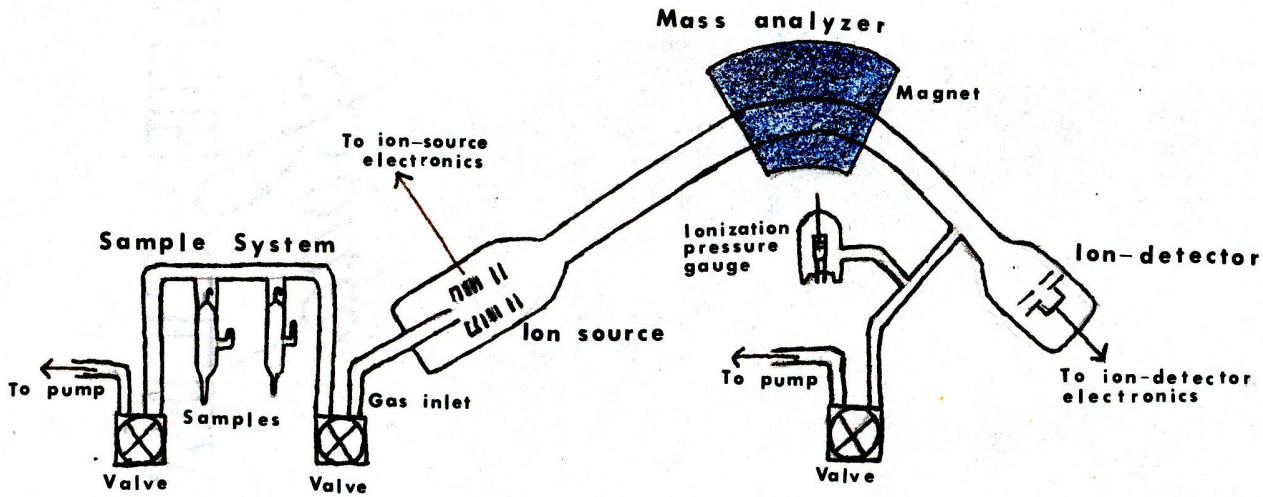

Figure 3

Schematic diagram of a mass spectrometer for argon analysis.

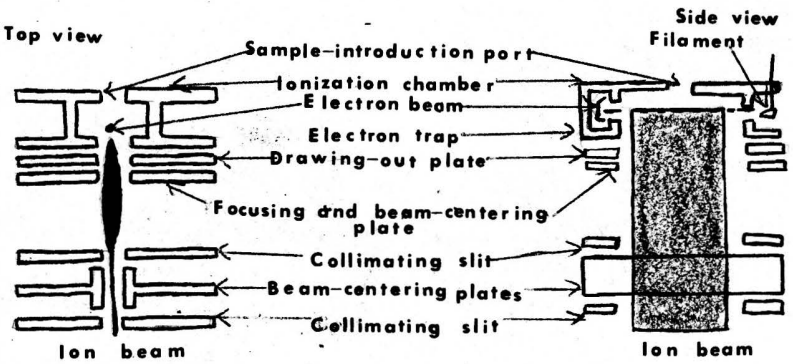

Figure 4

Schematic diagram of an electron-bombardment ion source.

the drawing-out plate and the chamber. As the beam of ions passes through the slits of the drawing-out plate, and of the collimating plates, it is accelerated and focused.

The accelerated beam of ions then enters the field of a large electromagnet, which separates the ions into curved paths with radii inversely proportional to the square roots of the charge to mass ratios. The radius of deflection can be altered by varying the accelerating voltage as well as the magnetic field strength.

After leaving the electromagnet, the separate beams travel down the analyzer tube toward the ion detector. Only one mass of ionized particles has the correct angle to go through the defining slit and hit the ion collection plate. As the argon ions strike the collector their charge is lost, as it is balanced by electrons. Electrons to balance the positive charge flow in from the ground across a resistor. The voltage generated across the terminals of the resistor is measured by a vibrating reed electrometer. The vibrating reed electrometer amplifies the voltage, which is then read on a strip-chart recorder. By varying the magnetic field of the analyzer, the curvature of the ion beams is changed. As a result the ^{36}Ar, ^{38}Ar, and ^{40}Ar beams consecutively pass through the slit and strike the collector plate for measurement.

Because the composition of atmospheric argon is known, and because the composition and quantity of spike argon are known, the quantity of ^{40}Ar can be determined through comparison of the peak heights recorded on the strip chart.

The fractions of ^{38}Ar and ^{40}Ar resulting from atmospheric contamination are calculated from the ratios of ^{36}Ar to ^{38}Ar and ^{40}Ar to ^{36}Ar in the atmosphere. Using these values and the known ratio ^{40}Ar to ^{38}Ar in the tracer, the quantity of radiogenic ^{40}Ar in the sample can be calculated by subtracting the atmospheric component from the total ^{40}Ar.

Potassium Analysis

The flame photometer utilizes the fact that the alkali metals, whether in compounds or uncombined, will emit their characteristic radiation when excited by an air flame. The technique used in the project was the lithium-internal-standard-method. In this method, the standard solutions are made by dissolving a known quantity of potassium salt to obtain the desired potassium concentration. Next, a known quantity of lithium, the internal standard, is added to both the unknown and the standard solutions. The flame photometer analyzes the solutions, and the intensity of the potassium radiation is indicated on a scale. The concentration of potassium in the unknown can be determined by comparison of the data from the unknown and known solutions because the lithium content of the unknown and standard solutions are the same, and because the potassium content of the standard solutions are known. The use of lithium as the internal standard lessens background interference from other elements.

The biotite was dissolved in a mixture of hot hydrofluoric, and sulfuric acid. The silicon is removed as SuF_4 through evaporation. The solution that remains is diluted,

and the internal standard (a known quantity of lithium) is added.

In the atomizer the unknown solution measured is drawn up in the wake of and mixed with compressed air. Furthermore, the larger droplets are separated and drained off in the atomizer. The atomized air and solution mixture is mixed with propane, and then conveyed to the burner (see Fig. 5).

The flame excites the potassium and lithium which begin to emit their characteristic radiations. The light is collected by the condenser, passed through the filters, and converted to an electric current by a photo-electric detector. The voltage produced is then indicated on a scale. The value on the scale is a measure of the concentration of the element in the solution. This is compared to the abundance of the element in standard solutions to determine their actual concentration.

PREVIOUS AGE DETERMINATION

Previous age determinations on the Hope Granite and associated dikes were done by the potassium-argon method (McDougall and Grindley, 1965). The ages obtained were middle and late Ordovician. Accuracy was better than $\pm$ 3%, and the reproducibility of the physical measurements was better than $\pm$ 2% (see Table 1).

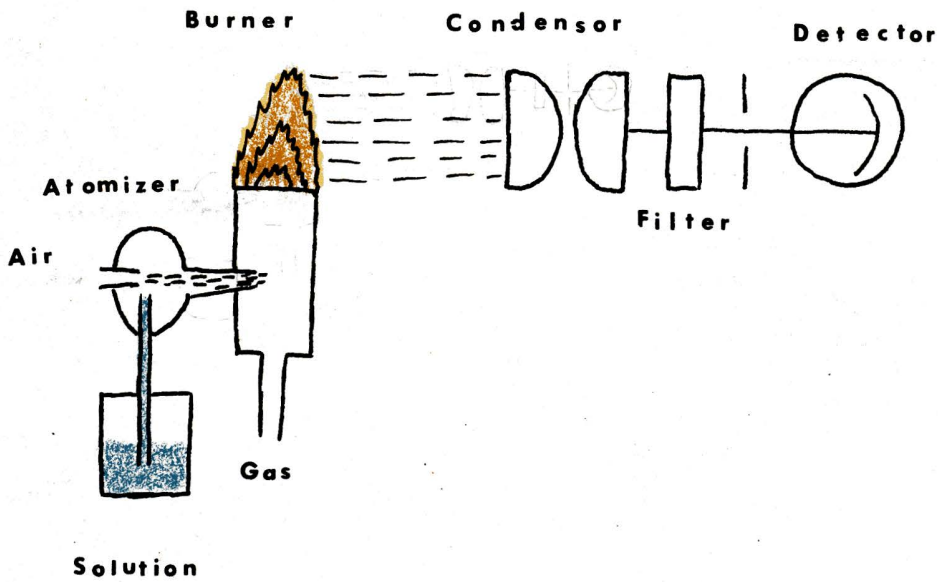

Figure 5

Schematic diagram of a flame photometer that uses a lithium internal standard.

Table 1

Location	Geologic Unit	Method and Material	Age (m.y.)
Miller Range 83°02'S., 157°43'E	Hope Granite	K-Ar Muscovite	478
Miller Range 83°06'S, 156°30'E	Lamprophrye Dike	K-Ar Biotite	476
Mouth of Beardmore Glacier 84°57'S, 172°30'E	Hope Granite	K-Ar Biotite	465,450
Miller Range 83°57'S, 157°30'E	Hope Granite	K-Ar Biotite	463

Table 2

Data used in potassium-argon age calculation by computer.

Potassium analysis		
	Percent K	7.019 %
	(W) Sample weight	0.07246 grams
Argon analysis		
	$(^{40}Ar/^{38}Ar)_U$ $^{40}Ar/^{38}Ar$ ratio in mixture before application of discrimination constant.	2.4721
	$(^{38}Ar/^{36}Ar)_U$ $^{38}Ar/^{36}Ar$ ratio in mixture before application of discrimination constant.	3311.9972
	$(^{40}Ar/^{38}Ar)_T$ $^{40}Ar/^{38}Ar$ ratio in tracer	0.0018
	$(^{38}Ar/^{36}Ar)_T$ $^{38}Ar/^{36}Ar$ ratio in tracer	$2.72X10^{-5}$
	$(^{40}Ar/^{38}Ar)_A$ $^{40}Ar/^{38}Ar$ ratio in atmosphere	1581
	$(^{36}Ar/^{38}Ar)_A$ $^{38}Ar/^{36}Ar$ ratio in atmosphere	5.32
	(D) Discrimination constant	0.995
	Scale 40	10 volts
	Scale 38	10 volts
	Scale 36	10^{-3} volts
	$(^{38}Ar_T)$ moles ^{38}Ar in traces	$2.213X10^{-10}$ moles
	λ_ϵ	$0.585X10^{-10}$/yr.
	λ_β	$4.72X10^{-10}$/yr.

POTASSIUM-ARGON AGE CALCULATION

The data used in the calculations are listed in Table 2.

A. Calculation of ^{40}K

1. Calculation of grams of K

$$K = (K \text{ fraction})(W)$$

$$= (.07019)(.07246 \text{ grams})$$

$$= .005086 \text{ grams}$$

2. Calculation of moles of ^{40}K

$$^{40}K = \frac{(\text{atoms } ^{40}K/\text{atoms K})(\text{grams K})}{(\text{grams K/mole K})}$$

$$= \frac{(1.19 \times 10^{-4})(.005086 \text{ grams})}{39.10 \text{ grams/mole}}$$

$$= 1.5479 \times 10^{-8} \text{ mole}$$

B. Calculation of $^{40}Ar_{rad}$.

1. Calculation of true $^{40}Ar/^{38}Ar$ and $^{38}Ar/^{36}Ar$ ratios in the gas mixture.

$$(^{40}Ar/^{38}Ar)_M = (^{40}Ar/^{38}Ar)_U \frac{(\text{scale } 40)}{(\text{scale } 38)} \frac{(40 \text{ scale correction factor})}{(38 \text{ scale correction factor})}(D)$$

$$= (2.4721)(.995)$$

$$= 2.4597$$

$$(^{38}Ar/^{36}Ar)_M = (^{38}Ar/^{36}Ar)_U \frac{(\text{scale } 38)}{(\text{scale } 36)} \frac{(38 \text{ scale correction factor})}{(36 \text{ scale correction factor})}(D)$$

$$= (3311.9972)(.995)$$

$$= 3295.4372$$

2. Calculation of total moles of ^{40}Ar

$$^{40}Ar_{total} = (^{40}Ar/^{38}Ar)_M \ (^{38}Ar_T)$$

$$= (2.4597)(2.213\times10^{-10}\text{moles})$$

$$= 5.4433 \times 10^{-10}\text{moles}$$

3. Calculation of moles of $^{40}Ar_{rad.}$

$$^{40}Ar_{rad.} = {}^{38}Ar_T \left\{(^{40}Ar/^{38}Ar)_M \ (^{40}Ar/^{38}Ar)_T - \left[\frac{1-(^{38}Ar/^{36}Ar)_M(^{36}Ar/^{38}Ar)_T}{(^{38}Ar/^{36}Ar)_M(^{36}Ar/^{38}Ar)_A-1}\right] \times \left[(^{40}Ar/^{38}Ar)_A - (^{40}Ar/^{38}Ar)_M\right]\right\}$$

$$= (2.213\times10^{-10}\text{mole}) \ (2.4597)-(.0018) - \left[\frac{1-(3312)\ 2.72\times10^{-5}}{(3312)\ (5.32)-1}\right]\left[(1581)-(2.4597)\right]\}$$

$$= 5.2581\times10^{-10}\text{moles}$$

4. Calculation of percentage of $^{40}Ar_{rad.}$

$$\text{Percent } ^{40}Ar_{rad.} = \frac{100(^{40}Ar_{rad.})}{(^{40}Ar_{total})}$$

$$= \frac{100(5.2581\times10^{-10}\text{moles}}{(5.4433\times10^{-10}\ \text{moles})}$$

$$= 96.6\%$$

C. Calculation of apparent age

$$t = \frac{1}{\lambda_\epsilon+\lambda_\beta}\log_e\left[\frac{^{40}Ar_{rad.}}{^{40}K}\frac{\lambda_\epsilon+\lambda_\beta}{\lambda_\epsilon}+1\right]$$

$$= 1.885\times10^9 \ \log_e\left[(9.068\ \frac{^{40}Ar_{rad.}}{^{40}K} + 1\right]$$

$$= 1.885\times10^9 \ \log_e\left[(9.068(\frac{5.2581\times10^{-10}\text{moles})}{(1.5479\times10^{-8}\text{moles}} + 1\right]$$

$$= 1.885\times10^9 \ \log_e\left[9.068\ (3.3975\times10^{-2}) + 1\right]$$

$$= 5.06.25 \text{ million years}$$

DISCUSSION OF RESULTS

The age of the sample resulting from the potassium-argon determination is 506 million years, with 1.12 percent standard deviation, or plus or minus 6 million years. This would appear to be satisfactory precision. However, the 1.12 percent standard deviation does not mean that the apparent age of the rock is necessarily accurate. The other ages obtained from samples of the Hope Granite are from 20 to 50 million years younger than the date obtained for this sample. (see Table 1); but that does not mean that either the age of this sample or the ages in Table 1 are necessarily incorrect. The biotite of the intrusive body from which the sample was taken may have crystallized sooner than the biotite dated by McDougall and Grindley. Or, the intrusive body from which this sample was taken may represent the beginning of the period of intrusion, while the other samples of Hope Granite may represent a slightly later phase of the period of intrusion. If the measured potassium content were lower than the actual potassium content of the sample the apparent age of the rock would be too old. Since this very problem has been noted previously as a result of erratic behavior of the flame photometer, this is a definite possibility.

Since the standard deviation for the $^{40}Ar/^{38}Ar$ and $^{38}Ar/^{36}Ar$ ratios is less than one percent, these two ratios can be considered to have satisfactory precision, and to have little adverse affect on the accuracy of the age determination. The atmospheric argon does not affect the accuracy or

the precision of the apparent age either. The percentage of atmospheric argon present is 3.4%. An uncertainty in the atmospheric ^{40}Ar content would have to be quite large to affect the accuracy and precision appreciably, since the quantity of atmospheric ^{40}Ar present is so small compared to the quantity of radiogenic ^{40}Ar present.

The precision of the potassium analysis of the sample was quite unsatisfactory, and the uncertainty may be as high as 5 percent. The flame photometer was not operating properly at the time of the potassium analysis, and a considerable error may have been introduced into the age-determination at that time. It is believed that the potassium content may have been underestimated. If the observed potassium content is too low by 5 percent, the date would be too great by 20 million years (see Table 4).

Table 3

Results of potassium-argon age determination

K (%)	^{40}K moles	$^{40}Ar_{rad.}$ moles	$\frac{^{40}Ar_{rad.}}{^{40}K}$
7.019	1.5477×10^{-8}	5.2582×10^{-10}	3.3975×10^{-2}

$^{40}Ar_{rad.}$ (%)	Apparent age (m.y.)	Standard Dev. (m.y.)	Percent St.Dev.
99.6	506.3±25	5.7	1.12

$\frac{\%\ 40}{\sigma 38}$	$\frac{\%\ 38}{\sigma 36}$
0.0833	0.3385

Later redetermination of K^+ gives 7.356 %, giving age of 479 m.y.
R. J. Fleck

Table 4

Ages resulting from error in potassium analysis

K (%)	^{40}K moles	$\frac{^{40}Ar_{rad.}}{^{40}K}$	Apparent age (m.y.)
7.019	1.5477×10^{8}	3.39×10^{-2}	506
7.50	1.63×10^{-8}	3.23×10^{-2}	480
8.00	1.74×10^{-8}	3.02×10^{-2}	452

REFERENCES

1. Dalrymple, G. B., and Lanphere, M. A., 1969, Potassium-Argon Dating: San Francisco, W. H. Freeman and company.

2. Grindley, G. W., 1963, The Geology of The Queen Alexandra Range, Beardmore Glacier Dependency, Antarctica; with notes on the correlation of Gondwana sequences: New Zealand Journal of Geology and Geophysics, v. 6, p. 307-347.

3. Grindley, G. W., and Laird, M. G., 1969. Geology of the Shackleton Coast; Geologic Map of Antarctica, Shackleton Coast, Plate XIV Folio 12- Geology, Antarctic Map Folio Series; Amercial Geographical Society.

4. Grindley, G. W., McGreagor, V. R.; Walcott, R. I., 1964: Outline of the Geology of the Nimrod-Beardmore-Axel Heiberg Region, Ross Dependency, Antarctica. In "Antarctic Geology" North Holland, Amsterdam.

5. Grindley, G. W.; Warren, G., 1969: Stratigraphic Nomenclature and Correlation in the Western Ross Sea Region Antarctic. In "Antarctic Geology" North Holland, Amsterdam.

6. Hamilton, E. I., 1965, Applied Geochronology: New York, Academic Press.

7. Laird, M. G., 1963, Geomorphology and Stratigraphy of the Nimrod Glacier-Beaumont Bay Region, Southern Victoria Land, Antarctica: New Zealand Journal of Geology and Geophysics, v. 6, p. 465-484.

8. McDougall, I., and Grindley, G. W., 1965, Potassium Argon Dates on micas from the nimrod-Beardmore-Axel Heiberg Region, Ross Dependency, Antarctica: New Zealand Journal of Geology and Geophysics, v. 8, p. 304-313.